

Effective Monkey Saddle Points and Berry and Lever Mechanisms in the Topomerization of SF₄ and Related Tetracoordinated AX₄ Species

Michael Mauksch[†] and Paul von Ragué Schleyer^{*,†,‡}

Computer Chemie Centrum, Universität Erlangen-Nürnberg, Nögelsbachstrasse 25, 91052 Erlangen, Germany, and Computational Chemistry Annex, University of Georgia, Athens, Georgia 30602-2525

Received May 7, 1999

The topomerization mechanisms of the SF₄ and SCl₂F₂ sulfuranes, as well as their higher (SeF₄, TeF₄) and isoelectronic analogues PF₄⁻, AsF₄⁻, SbF₄⁻, SbCl₄⁻, ClF₄⁺, BrF₄⁺, BrCl₂F₂⁺, and IF₄⁺, have been computed at B3LYP/6-31+G* and at B3LYP/6-311+G*. All species have trigonal bipyramidal (TBP) C_{2v} ground states. In such four-coordinated molecules, Berry rotation exchanges both axial with two equatorial ligands simultaneously while the alternative “lever” mechanism exchanges only one axial ligand with one equatorial ligand. While the barrier for the lever exchange in SF₄ (18.8 kcal mol⁻¹) is much higher than that for the Berry process (8.1 kcal mol⁻¹), both mechanisms are needed for complete ligand exchange. The F_{ax}F_{ax} and F_{eq}F_{eq} isomers of SF₂Cl₂ have nearly the same energy and readily interconvert by BPR with a barrier of 7.6 kcal mol⁻¹. The enantiomerization of the F_{ax}F_{eq} chiral isomer can occur by either the Berry process (transition state barrier 8.3 kcal mol⁻¹) or the “lever” mechanism via either of two C_s transition states, based on the TBP geometry: Cl_{ax} ↔ Cl_{eq} or F_{ax} ↔ F_{eq} exchanges with barriers of 6.3 and 15.7 kcal mol⁻¹, respectively. Full scrambling of all ligand sites is possible only by inclusion of the lever mechanism. Planar, “tetrahedral”, and triplet forms are much higher in energy. The TBP C_{3v} structures of AX₄ either have two imaginary frequencies (NIMAG = 2) for the X = F, Cl species or are minima (NIMAG = 0) for the X = Br, I compounds. These “effective monkey saddle points” have degenerate modes with two small frequencies, imaginary or real. Although a strictly defined “monkey saddle” (with degenerate frequencies exactly zero) is not allowed, the flat C_{3v} symmetry region serves as a “transition state” for trifurcation of the pathways. The BPR mechanism also is preferred over the alternative lever process in the topomerization of the selenurane SeF₄ (barriers 5.9 vs 12.1 kcal mol⁻¹), the tellurane TeF₄ (2.1 vs 6.4), and the interhalogen cations ClF₄⁺ (2.5 vs 14.8), BrF₄⁺ (4.7 vs 11.3), BrF₂Cl₂⁺ (14.6 vs 17.4), and IF₄⁺ (1.4 vs 6.0), as well as for the series PF₄⁻ (7.0 vs 9.0), AsF₄⁻ (9.3 vs 17.2), and SbF₄⁻ (3.8 vs 5.3 kcal mol⁻¹), all computed at B3LYP/6-311+G* with the inclusion of quasirelativistic pseudopotentials for Te, I, and Sb. The heavier halogens increasingly favor the lever process, where the barrier (2.6 kcal mol⁻¹) pertaining to the effective monkey saddle point (C_{3v} minimum for SbCl₄⁻) is less than that for the Berry process (8.2 kcal mol⁻¹).

1. Introduction

First reported in 1911, SF₄,¹ the prototypical sulfurane, has a C_{2v} structure. This can be based on a trigonal bipyramid (TBP) with one equatorial site vacant.^{2,3} An alternative C_{3v} form, with a missing axial site, also can be based on TBP but is expected to be higher in energy. This would comply with the VSEPR model,⁴ which favors structures with equatorial lone pairs in which the bond–lone pair repulsion is minimized.⁴

Indeed, the low-temperature NMR of SF₄ shows two fluorine signals of equal area.^{5–14} Like other sulfuranes, SF₄ is a nonrigid

molecule which undergoes rapid exchange of ligand positions as revealed by its dynamic NMR spectra at higher temperatures.⁵ Muetterties and Phillips showed in 1957⁶ that the 30 MHz ¹⁹F NMR spectrum of SF₄ coalesces at -47 °C into a single broad resonance which gradually sharpens to a narrow singlet at higher temperatures.⁶ However, accurate measurements of the topomerization barrier were complicated for many years from difficulties due to impurities^{6a,7} and to the intervention of bimolecular

* Author to whom correspondence should be addressed. E-mail: schleyer@uga.edu.

[†] Universität Erlangen-Nürnberg.

[‡] University of Georgia.

- (1) Ruff, O.; Heinzelmann, A. *Z. Anorg. Allg. Chem.* **1911**, 72, 63.
- (2) (a) Tolles, W. M.; Gwinn, W. D. *J. Chem. Phys.* **1962**, 36, 1119. (b) Kimura K.; Bauer, S. H. *J. Chem. Phys.* **1963**, 39, 3172.
- (3) In contrast, a C_{4v} global minimum had been predicted at MP2/DZP and QCISD(T)/DZP levels for SH₄: Marsden, C. J.; Smart, B. A. *Aust. J. Chem.* **1994**, 47, 1431. Also see: Wittkopp, A.; Prall, M.; Schreiner, P. R.; Schaeffer III, W. F. *Phys. Chem. Chem. Phys.*, **2000**, 2, 2239. The most recent paper on SF₄ is: Drozdova, Y.; Steudel, R.; Koch, W.; Miasiewicz, K.; Topol, I. A. *Chem. Eur. J.* **1999**, 5, 1936.
- (4) Gillespie, R. J. *Molecular Geometry*; Van Nostrand Reinhold: London, 1972.

- (5) Pople, J. A.; Schneider, W. G.; Bernstein, H. J. *High-resolution Nuclear Magnetic Resonance*; McGraw-Hill: New York, 1959; p 223.
- (6) (a) Muetterties, E. L.; Phillips, W. D. *J. Am. Chem. Soc.* **1959**, 81, 1084. (b) Muetterties, E. L.; Phillips, W. D. *J. Am. Chem. Soc.* **1957**, 79, 322.
- (7) Muetterties, E. L.; Phillips, W. D. *J. Chem. Phys.* **1967**, 46, 2861.
- (8) Cotton, F. A.; George, J. W.; Waugh, J. S. *J. Chem. Phys.* **1958**, 28, 944.
- (9) Gibson, J. A.; Ibbot, D. G.; Jansen, A. F. *Can. J. Chem.* **1973**, 51, 3203.
- (10) Lewin, I. W.; Harris, W. C. *J. Chem. Phys.* **1971**, 55, 3048.
- (11) Bacon, J.; Gillespie, R. J.; Quali, J. W. *Can. J. Chem.* **1963**, 41, 1016.
- (12) Darragh, J. I.; Sharp, D. W. A. *Angew. Chem., Int. Ed. Engl.* **1970**, 9, 73.
- (13) Klemperer, W. G.; Krieger, J. K.; McCreary, M. D.; Muetterties, E. L.; Traficante, D. D.; Whitesides, G. M. *J. Am. Chem. Soc.* **1975**, 97, 7023.
- (14) Seel, F.; Gombler, W. J. *J. Fluorine Chem.* **1974**, 4, 327.

reactions,^{6a,8} and by conflicts in the interpretation of data. Consequently, experimentally determined activation energies for the intramolecular rearrangement^{15–19} of SF₄ range from 4.6⁸ (for intermolecular exchange) to 16 kcal mol⁻¹⁹ as deduced from the calculation of the NMR relaxation times from the signal coalescence temperatures at different temperatures. A barrier of 10 kcal mol⁻¹ was obtained from IR studies in 1971 by a fitting of the potential function for the vibrational mode pertaining to the angle distortion between equatorial fluorines.¹⁰ More recent measurements at different gas pressures gave values in a much narrower range, from 11.7¹⁴ to 13.7²⁰ kcal mol⁻¹; 11.2 kcal mol⁻¹¹⁴ was deduced in the liquid phase.

These values are consistent with computed barrier heights for the BPR process in SF₄, 10.6 kcal mol⁻¹ at HF/6-31G^(*)^{19a} (the 6-31G* basis set was used for S), 10.3 kcal mol⁻¹ at MP2/DZP, and 9.0 kcal mol⁻¹ with an LSDA functional.^{19b} Density functional calculations consistently give values that are 2–4 kcal mol⁻¹ lower than the MP2/DZP results.²¹

Klemperer¹³ provided conclusive evidence in 1975 that “Berry pseudorotation” (BPR)^{16–18} was the mechanism by which the fluorines in SF₄ are interchanged. This mechanism, first proposed for ligand exchange in PF₅ in 1959^{16a} (eventually also verified by Klemperer et al. in 1975),¹³ results for such pentacoordinated systems in a total scrambling by a 5-fold repetition of the BPR topomerization step.²²

“Turnstile rotation” (TR) was proposed by Ugi and Ramirez as an alternative to BPR in five-coordinated systems.^{22b,c} The turnstile process involves an internal rotation of a ligand pair relative to the other three ligands in mutually opposite directions^{22,23} and, like BPR, results in a simultaneous exchange of both axial with two equatorial ligands in pentacoordinated compounds.²²

In tetraordinated compounds like SF₄ with an additional lone pair at the central atom, a single BPR or TR step either would result in a TBP minimum structure with three equatorial ligands and a vacant axial position or does not result in total scrambling of the ligand positions, since only a simultaneous pairwise exchange of both axial ligands with the equatorial ligands is involved.^{15,22} To achieve a full ligand scrambling in such SF₄-like systems without involving minima with vacant apical sites, Musher²⁴ and Minyaev and Minkin^{25,26} indepen-

dently considered several mechanistic alternatives, involving only single axial–equatorial exchange of ligands, in 1975.

The best alternative, termed the “lever” mechanism,^{25–28} was computed for SF₄ by Minkin and Minyaev at extended Hückel and CNDO/2 levels in 1975²⁵ (we located the transition state at B3LYP/6-311+G* in 1994).²⁸ This mechanism resembles in outcome two consecutive “turnstile” steps. However, in contrast to the TR, only three ligands rotate with respect to the remaining ligand and the central atom. As this mechanism involves a single axial–equatorial exchange of ligands, it would allow a total scrambling of all ligand positions.

Indeed, low-energy mechanisms for the enantiomerization of SABCD and SA₂BC chiral halosulfuranes, like **a**,²⁹ **b**,³⁰ and **c**³¹ in Scheme 1, appear to be absent, since such optically active sulfuranes^{29–34} could be resolved.³⁰ The ¹⁹F NMR data for **a** in solution is consistent with the presence of two nonequivalent sulfur-bound fluorines, because two signals are given by the two CF₃ groups.²⁹ A single Berry rotation step was considered for the F_{ax} ↔ F_{eq} exchange of the two fluorines,²⁹ but racemization of **a** was not observed.

Solutions of the similar compound, (*S*)-chlorosulfurane **b**,³⁰ racemize only slowly on standing at room temperature (the lower limit of the barrier of uncatalyzed racemization is 25 kcal mol⁻¹).³⁰ Martin and Balthazor anticipated the possibility of a five-step enantiomerization of **b** on the basis of the Berry process.³⁰ If the Berry process would afford racemization of **b**, why it does it not for **a**?

Similarly, in spirobicyclic sulfuranes like **d**³⁵ and **e**,³⁶ with identical axial and equatorial ligands, rapid interconversion of enantiomeric forms was observed (racemization barrier: 7.5 kcal mol⁻¹ at –100 °C).^{35,36} While **d** displays four ¹⁹F NMR peaks below –100 °C, only two F peaks appear above –100 °C.³⁵ But even at 200 °C no further coalescence to a single signal was observed, ruling out facile single axial–equatorial exchange of ligands.³⁵ Spirobicyclic **e** also enantiomerizes rapidly with an experimental barrier of 9 kcal mol⁻¹.³⁶ However, isomerization of **f**,³⁷ with an endo ethyl substituent, to the diastereomer with an exo ethyl substituent proceeds with a much higher barrier of 30 kcal mol⁻¹ at 84 °C! Why?

We decided that the problem of sulfurane racemization would be addressed best by studying a simple model for a chiral sulfurane computationally. Hence, we considered the (unknown) mixed sulfur halide SF₂Cl₂ in the present work.

The potential energy surface of the isoelectronic and isostructural ClF₄⁺ was examined recently at SCF/DZP and at MP2/DZP.²⁷ While the reported MP2 data was suspect (e.g., with a D_{4h} global minimum and a C_{3v} minimum, 79.6 kcal mol⁻¹ above

(15) Oae, S. *Organic Sulfur Chemistry: Structure and Mechanism*; CRC Press: Boca Raton, FL, 1991.

(16) (a) Berry, R. S. *J. Chem. Phys.* **1960**, *32*, 933. (b) Berry, J. S. *Rev. Mod. Phys.* **1960**, *32*, 447.

(17) Sheppard, W. A. *J. Am. Chem. Soc.* **1962**, *84*, 3058.

(18) Chen, M. M. L.; Hoffmann, R. *J. Am. Chem. Soc.* **1976**, *98*, 1647.

(19) (a) Minyaev, R. M.; Yudelevich, J. A. *J. Mol. Struct. (THEOCHEM)* **1992**, *262*, 73. (b) Ziegler, T.; Gutsev, G. L. *J. Chem. Phys.* **1992**, *96*, 7623.

(20) Spring, C. A.; True, N. S. *J. Am. Chem. Soc.* **1983**, *105*, 7231.

(21) (a) Christe, K. O.; Dixon, D. A.; Schrobilgen, G. J.; Wilson, W. W. *J. Am. Chem. Soc.* **1997**, *119*, 3918. (b) Christe, K. O.; Dixon, D. A.; Mercier, P. A.; Sanders, J. C. P.; Schrobilgen, G. J.; Wilson, W. W. *J. Am. Chem. Soc.* **1994**, *116*, 2850.

(22) (a) Gillespie, P.; Hoffmann, P.; Klusacek, H.; Marquarding, D.; Pfohl, S.; Ramirez, F.; Tsolis, E. A.; Ugi, I. *Angew. Chem.* **1971**, *83*, 691. (b) Ugi, I.; Marquarding, D.; Klusacek, H.; Gokel, G.; Gillespie, P. *Angew. Chem.* **1970**, *82*, 741. (c) Ramirez, F.; Ugi, I. In *Advances in Physical Organic Chemistry*; Gold, V., Ed.; Academic Press: London, 1971; Vol. 9, p 25.

(23) For theoretical studies, see: (a) Wasada, H.; Hirao, K. *J. Am. Chem. Soc.* **1992**, *114*, 16. (b) Wang, P.; Agrafiotis, D. K.; Streitwieser, A.; Schleyer, P. v. R. *J. Chem. Soc., Chem. Commun.* **1990**, *79*, 201. (c) Shih, S.; Peyerimhoff, S. D.; Bunker, R. *Theor. Chim. Acta* **1978**, *389*.

(24) Musher, J. I.; Cowley, A. H. *Inorg. Chem.* **1975**, *14*, 2302.

(25) Minkin, V. I.; Minyaev, R. M. *Zh. Org. Khim. (USSR)* **1975**, *10*, 1993 (p 2023 in English translation).

(26) Minyaev, R. M.; Minkin, V. I. *Zh. Strukt. Khim. (USSR)* **1977**, *18*, 274 (p 220 in English translation).

(27) Minyaev, R. M.; Wales, D. J. *J. Chem. Soc., Faraday Trans.* **1994**, *90*, 1831.

(28) In ref 27, Minyaev acknowledged that “the true transition state for the lever mechanism (in SF₄)...has been found by Schleyer et al.” in Erlangen.

(29) Martin, L. D.; Perozzi, E. F.; Martin, J. C. *J. Am. Chem. Soc.* **1979**, *101*, 3595.

(30) Martin, J. C.; Balthazor, T. M. *J. Am. Chem. Soc.* **1977**, *99*, 152.

(31) Martin, J. C.; Perozzi, E. F. *J. Am. Chem. Soc.* **1974**, *96*, 3155.

(32) Balthazor, T. M.; Martin, J. C. *J. Am. Chem. Soc.* **1975**, *97*, 5634.

(33) (a) Nudelman, A. *The chemistry of optically active sulfur compounds*; Gordon and Breach Science Publ.: New York, 1984. (b) Volatron, F. *J. Mol. Struct. (THEOCHEM)* **1989**, *186*, 167.

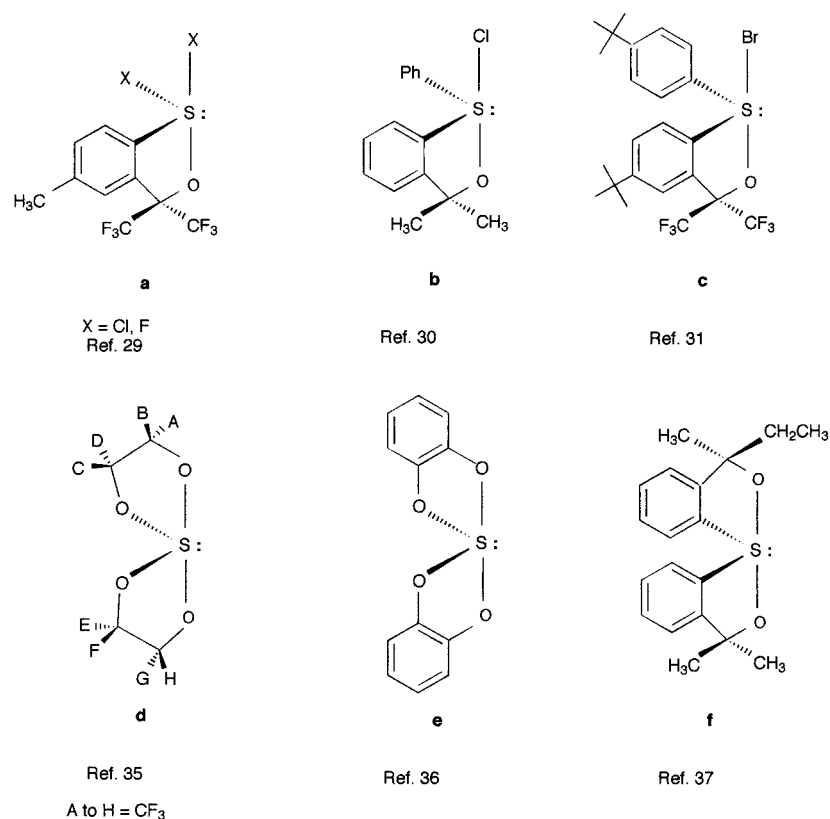
(34) Hayes, R. A.; Martin, J. C. In *Organic Sulfur Chemistry*; Bernardi, F., Csizmadia, I. G., Mangini, A., Eds.; Elsevier: Amsterdam, 1985.

(35) Astrologes, G. W.; Martin, J. C. *J. Am. Chem. Soc.* **1976**, *98*, 2895.

(36) Belkind, B. A.; Denney, D. B.; Denney, D. Z.; Hsu, Y. F.; Wilson, G. E. *J. Am. Chem. Soc.* **1978**, *100*, 6327.

(37) Adzima, L. J.; Martin, J. C. *J. Org. Chem.* **1977**, *42*, 4006.

Scheme 1



the C_{2v} minimum), the reported activation barrier for the BPR process in ClF_4^+ is $6.7 \text{ kcal mol}^{-1}$, and $39.5 \text{ kcal mol}^{-1}$ for the lever mechanism (with a C_s transition state based on the TBP geometry) at SCF/DZP and with sequential axial–equatorial exchange of fluorine atoms. In C_{3v} , a second-order saddle point was found on a flat hilltop, only $0.6 \text{ kcal mol}^{-1}$ (at the SCF/DZP level) higher in energy than the lever TS.²⁷ Gradient lines, corresponding to the imaginary frequencies of that C_{3v} stationary point, were supposed to connect to three permutational isomers of the C_s TS's and the C_{2v} minima.

As pseudorotation also has been observed in arsenanes,^{38,39} selenuranes,⁴⁰ and PF_4^- (the computed barrier at MP2/DZP, 10.2, agrees with the $10.3 \text{ kcal mol}^{-1}$ observed experimentally),²¹ we extended our investigation to known members of the isoelectronic series: SF_4 , SeF_4 ,^{41,42} TeF_4 ,⁴³ ClF_4^+ ,^{44,45} BrF_4^+ ,⁴⁵ IF_4^+ ,⁴⁵ PF_4^- ,²¹ AsF_4^- ,⁴⁶ and SbF_4^- .⁴⁷ For comparison, we have also studied the related $\text{BrF}_2\text{Cl}_2^+$ system and the SbCl_4^- anion, to seek possible trends in the topomerization barriers for related systems.

Questions we answer in the present work are: Why do some optically active sulfuranes isomerize rapidly while others do

Table 1. Total Energies (hartree) and Zero Point (ZPE) and ZPE-Corrected Relative Energies (kcal mol^{-1}) of SF_4 Species at the (U)B3LYP/6-31+G* and CCSD(T)/6-31G* Levels^a

structure ^b	NIMAG	sym	E_{tot}	E_{rel}	ZPE
1	(0)	C_{2v}	-797.49964 -795.99458 ^c	0.0	6.8
2	(1)	C_{4v}	-797.48647 -795.98009 ^c	8.1	6.8
3	(1)	C_s	-797.46978	18.8	5.9
4	(2)	D_{4h}	-797.39907	62.7	4.7
5^d	(0)	D_{4h}	-797.41289	53.5	5.8
6	(2)	C_{3v}	-797.46913	19.2	5.7
7	(2)	C_{3v}	-797.42591	46.3	4.8
8	(3)	T_d	-797.41082	55.7	3.5

^a The number of imaginary frequencies (NIMAG) is given in parentheses. ^b See Figure 1 (for species **1–4** and **6–8**). ^c At the CCSD(T)/6-31G* level. ^d Triplet, run at UB3LYP/6-31+G*.

not? We invoke the lever mechanism for explanation. Which of the two mechanisms, Berry and lever, governs the topomerizations in SF_4 -like systems? While the Berry process always is lower in energy, the combination of both mechanisms is necessary to achieve complete ligand exchange.

2. Computational Methods

The GAUSSIAN-94 program⁴⁸ was employed for geometry optimizations at B3LYP/6-31+G* (for all stationary points in the SF_4 and SbCl_2F_2 systems, Tables 1 and 2) and at the B3LYP/6-311+G** DFT

- (38) Muetterties, E. L. *Rec. Chem. Prog.* **1970**, *31*, 51.
 (39) Holmes, R. R. *Acc. Chem. Res.* **1972**, *5*, 296.
 (40) Lindgren, B. *Acta Chem. Scand.* **1972**, *26*, 2560.
 (41) Seppelt, K. *Z. Anorg. Allg. Chem.* **1975**, *416*, 12.
 (42) (a) Damerius, R.; Huppmann, P.; Lentz, D.; Seppelt, K. *J. Chem. Soc., Dalton Trans.* **1989**, 2821. (b) Angyan, J. G.; Csizmadia, I. G.; Daudel, R.; Poirier, R. A. *Chem. Phys. Lett.* **1986**, *131*.
 (43) Carre, J.; Germain, P.; Thourey, J.; Perachon, G. *J. Fluorine Chem.* **1986**, *31*, 241.
 (44) Wilson, W. W.; Christe, K. O. *J. Fluorine Chem.* **1982**, *21*, 7.
 (45) Tornieporth-Oetting, I. C.; Klapötke, T. M. *Heteroat. Chem.* **1993**, *4*, 543.
 (46) Zhang, X.; Seppelt, K. *Z. Anorg. Allg. Chem.* **1997**, *623*, 491.
 (47) Chitsaz, S.; Dehnicke, K.; Frenzen, G.; Pilz, A.; Müller, U. *Z. Anorg. Allg. Chem.* **1996**, *12*, 2016.

- (48) Binkley, J. S.; Whiteside, R. A.; Raghavachari, K.; DeFrees, D. J.; Schlegel, H. B.; Frisch, M. J.; Fox, D. J.; Trucks, G. W.; Kahn, L. R.; Martin, R. L.; Gonzalez, C.; Seeger, R.; Gill, P. M. W.; Johnson, B. G.; Cheeseman, J. R.; Robb, M. A.; Keith, T.; Montgomery, J. A.; Stefanov, B. B.; Challacombe, M.; Peng, C. Y.; Ayala, P. Y.; Chen, W.; Wong, M. W.; Andres, J. L.; Replogle, E. S.; Gomperts, R.; Baker, J.; Stewart, J. P.; Head-Gordon, M.; Al-Laham, M. A.; Zakrzewski, V. G.; Cioslowski, J.; Ortiz, J. V.; Foresman, J. B.; Nanayakkara, A.; Petersson, G. A.; Pople, J. A. *GAUSSIAN 94*, revision C.3; Gaussian, Inc.: Pittsburgh, PA, 1995.

Table 2. Total Energies at B3LYP/6-31+G* (hartree) and Zero Point (ZPE) and ZPE-Corrected Relative Energies (kcal mol⁻¹) (in Square Brackets) of SCl₂F₂ Species^a

structure ^b	NIMAG	sym		E_{tot}	ZPE
9	(0)	C_{2v}	F _{ax}	-1518.19543 [0.0]	4.9
10	(0)	C_{2v}	Cl _{ax}	-1518.19296 [2.2]	5.1
11	(0)	C_1		-1518.19179 [2.4]	5.0
12	(1)	C_s	F _{ax}	-1518.18047 [8.7]	4.4
13	(1)	C_s	Cl _{ax}	-1518.16550 [18.1]	4.1
14	(1)	C_s		-1518.17851 [10.7]	5.0
15	(1)	C_{2v}		-1518.09312 [63.8]	4.5
16	(1)	C_{2v}		-1518.18075 [9.2]	4.9
17	(1)	C_1	Cl _{ax}	-1518.16562 [17.8]	4.0
18	(2)	C_{2v}		-1518.11114 [52.2]	4.2
19	(2)	D_{2h}		-1518.12240 [44.4]	3.5
20	(3)	C_s		-1518.14769 [28.0]	2.9

^a The number of imaginary frequencies (NIMAG) is given in parentheses. ^b See Figure 6.

Table 3. Relative Energies for the Lever and BPR Mechanisms in Interhalogen Cations ClF₄⁺, BrF₄⁺, and BrF₂Cl₂⁺, Computed at B3LYP/6-31+G*, Including ZPE Corrections at the Same Level^a

system	species	NIMAG	sym	E_{rel}
ClF ₄ ⁺	21	0	C_{2v}	0.0
	22 lever	1	C_s	14.8
	23 BPR	1	C_{4v}	2.5
	24	2	C_{3v}	2.5
	25	2	D_{4h}	50.5
	26	3	D_{2d}	45.2
BrF ₄ ⁺	27	0	C_{2v}	0.0
	28 lever	1	C_s	11.3
	29 BPR	1	C_{4v}	4.7
	30	2	D_{4h}	76.3
	31	0	C_{2v}	0.0
BrF ₂ Cl ₂ ⁺	32	0	C_1	11.3
	33 lever	1	C_s	17.4
	34 lever	1	C_1	20.5
	35 BPR	1	C_s	14.6
	36	2	D_{2h}	36.0

^a The number of imaginary frequencies (NIMAG) and point group symmetries are given.

level (for the C_{2v} , C_s , C_{4v} and C_{3v} stationary points of SF₄, Table 1, of ClF₄⁺, Table 3, and of PF₄⁻, Table 5). CCSD(T)⁴⁹ single-point computations are reported on the B3LYP/6-31+G* geometries of SF₄ (Table 1). Hay and Wadt⁵⁰ pseudopotentials (which include a relativistically fitted effective core potential (RECP) for the core and inner valence electrons), in combination with the 6-311+G* basis set, have been applied for the valence shells of Se, Te, As, Sb, and I and all electrons on F (Table 5). The reliability of combining B3LYP with the RECP + DZVP basis was checked for TeCl₄ in 1998 and has been found satisfactory, although not as good as the combination of other methods and basis sets.⁵¹ To assess the validity of the "mixed" basis

Table 4. Comparison of Transition States for the Lever and BPR Mechanisms in the Tetrafluorophosphate Anion PF₄⁻, Computed at B3LYP/6-31+G* and B3LYP/6-311+G* Including ZPE Corrections of the Relative Energies at the Same Level^a

species	NIMAG	sym	E_{rel}	E_{exp}
37	0	C_{2v}	0.0	
	0		-741.05718 ^b	0.0
38 lever	1	C_s	16.1	
	1		-741.03119 ^b	16.3
39 BPR	1	C_{4v}	9.3	10.3 ^c
	1		-741.04118 ^b	10.0
40	2	C_{3v}	17.2	
	2		-741.02959 ^b	17.3
41	2	D_{4h}	54.5	
42	3	D_{2d}	50.2	

^a The number of imaginary frequencies (NIMAG) and point group symmetries are given. ^b B3LYP/6-311+G* level. ^c Reference 42.

Table 5. Comparison of Relative Energies at B3LYP/6-311+G* (kcal mol⁻¹) (without ZPE Corrections) of C_{2v} Minima, C_{4v} (Berry) and C_s (Lever) Transition States, and C_{3v} "Effective Monkey Saddle Points" on the Potential Energy Surfaces of Isoelectronic Tetracoordinated Species with a Central Atom from Group 15, 16, or 17^a

system	E_{rel}			
	C_{2v}	C_{4v}	C_{3v}	C_s
PF ₄ ⁻	0.0(0)	9.3(1)	17.2(2)	16.1(1)
AsF ₄ ⁻	0.0(0)	7.0(1)	9.0(2)	9.0(1)
SbF ₄ ^{-b}	0.0(0)	3.8(1)	5.3(0)	5.3(1)
SbCl ₄ ^{-c}	0.0(0)	8.2(1)	2.6(2)	2.6(1) ^d
SF ₄	0.0(0)	8.2(1)	19.1(2)	18.7(1)
SeF ₄	0.0(0)	5.9(1)	12.1(2)	12.0(1)
TeF ₄ ^b	0.0(0)	2.1(1)	6.4(2)	6.5(1)
ClF ₄ ⁺	0.0(0)	2.4(1)	15.6(2)	15.6(1) ^e
BrF ₄ ⁺	0.0(0)	4.8(1)		12.0(1)
IF ₄ ^{++b}	0.0(0)	0.0(1) ^f	6.0(0)	6.5(1)
IF ₄ ^{++c}	0.0(0)	1.4(1)		8.8(1)

^a The number of imaginary frequencies (determining the nature of the stationary points) is given in parentheses. ^b LANL2DZ basis set on the heavy element, 6-31+G* basis set on F. ^c Quasirelativistic ECP on all atoms, see ref 52. ^d ΔE to the C_{3v} form 3×10^{-3} kcal mol⁻¹. ^e The difference in energy (ΔE) to the C_{3v} form is less than 0.04 kcal mol⁻¹. ^f ΔE to the C_{2v} form is less than 0.01 kcal mol⁻¹.

set, we carried out additional computations on IF₄⁺ and SbCl₄⁻ by use of a large-core quasirelativistic pseudopotential (fitted to atomic properties, rather than relativistic all-electron Dirac-Fock calculations)⁵² on all atoms in combination with DZP valence shell basis sets.⁵³ Analytical second derivative calculations,⁵⁴ performed with GAUSSIAN 94 (G94) using standard basis sets and with GAUSSIAN 98⁵⁵ for the computations with pseudopotentials, established the nature of all stationary points at the respective level. The corresponding zero point energies (ZPE) were used to correct the relative energies of the SF₄ and SCl₂F₂ species. Intrinsic reaction coordinate (IRC)⁵⁶ calculations have been carried out with G94 (bond angle data of intermediate structures along the IRC path are given in Table A in the Supporting Information).

3. Results and Discussion

Sulfuranes. SF₄. The computed bond angles of the C_{2v} isomer of SF₄, **1** (Figure 1), are in close agreement with the electron diffraction⁵⁷ and microwave data (SF_{ax} 1.646 Å, SF_{eq} 1.545 Å, $\angle F_{\text{eq}}\text{SF}_{\text{eq}} = 101.6^\circ$, $\angle F_{\text{ax}}\text{SF}_{\text{ax}} = 173.1^\circ$ ⁵⁸). The computed bond

(49) (a) Bartlett, R. J.; Purvis, G. D. *Int. J. Quantum Chem.* **1978**, *14*, 516. (b) Pople, J. A.; Krishnan, R.; Schlegel, H. B.; Binkley, J. S. *Int. J. Quantum Chem.* **1978**, *14*, 545.

(50) (a) Hay, P. J.; Wadt, W. R. *J. Chem. Phys.* **1985**, *82*, 270. (b) Wadt, W. R.; Hay, P. J. *J. Chem. Phys.* p 284.

(51) Kovacs, A.; Csonka, G. I.; Keseru, G. M. *J. Comput. Chem.* **1998**, *19*, 308.

(52) Kuechle, W.; Dolg, M.; Stoll, H.; Preuss, H. *Mol. Phys.* **1991**, *74*, 1245.

(53) Kaupp, M.; Schleyer, P. v. R.; Stoll, H.; Preuss, H. *J. Am. Chem. Soc.* **1991**, *113*, 6012.

(54) Pulay, P. In *Ab initio methods in quantum chemistry*; Lawley, K. P., Ed.; Wiley: New York, 1987; p 241.

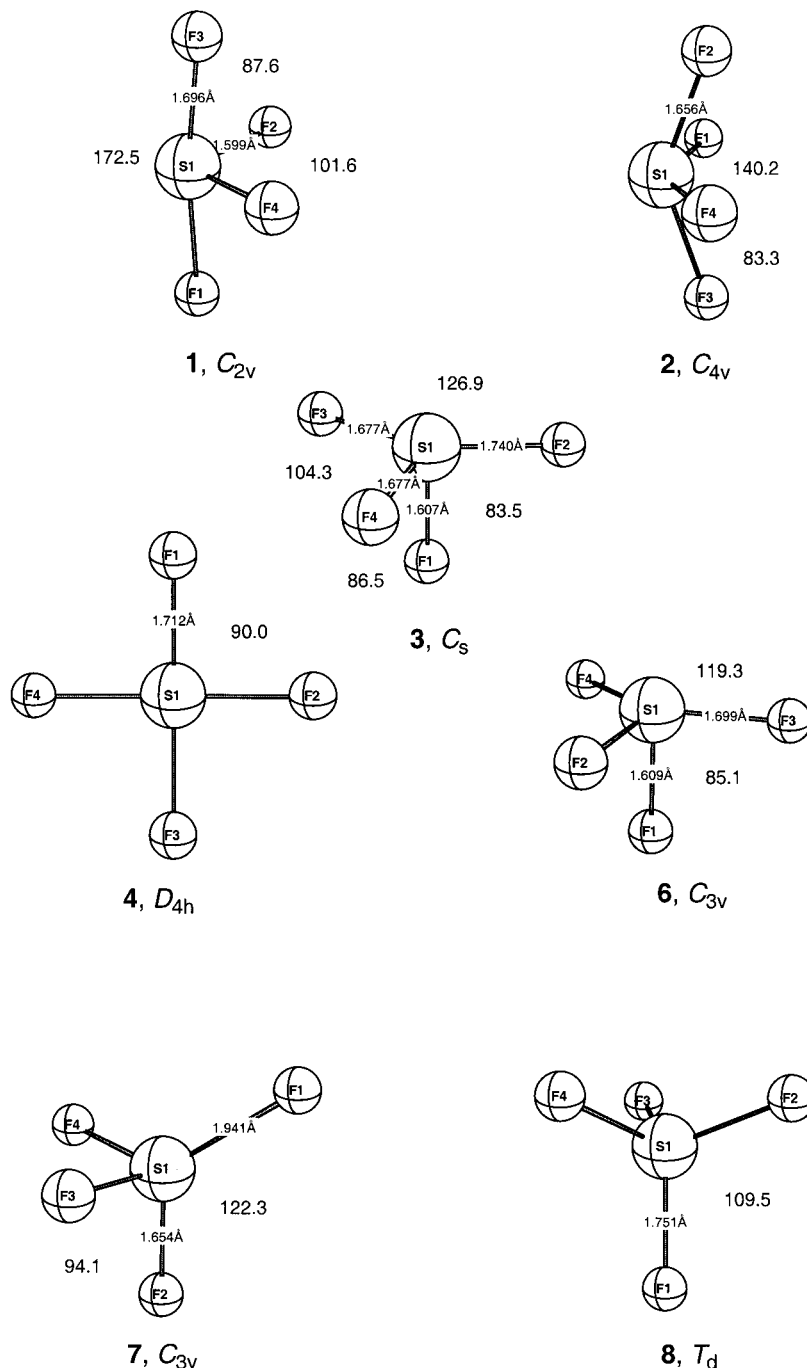


Figure 1. B3LYP/6-31+G* optimized structures of seven stationary points on the SF₄ PES.

lengths are somewhat longer (about 4%), than the experimental distances.

- (55) Frisch, M. J.; Trucks, G. W.; Schlegel, H. B.; Scuseria, G. E.; Robb, M. A.; Cheeseman, J. R.; Zakrzewski, V. G.; Montgomery, J. A., Jr.; Stratmann, R. E.; Burant, J. C.; Dapprich, S.; Millam, J. M.; Daniels, A. D.; Kudin, K. N.; Strain, M. C.; Farkas, O.; Tomasi, J.; Barone, V.; Cossi, M.; Cammi, R.; Mennucci, B.; Pomelli, C.; Adamo, C.; Clifford, S.; Ochterski, J.; Petersson, G. A.; Ayala, P. Y.; Cui, Q.; Morokuma, K.; Malick, D. K.; Rabuck, A. D.; Raghavachari, K.; Foresman, J. B.; Cioslowski, J.; Ortiz, J. V.; Stefanov, B. B.; Liu, G.; Liashenko, A.; Piskorz, P.; Komaromi, I.; Gomperts, R.; Martin, R. L.; Fox, D. J.; Keith, T.; Al-Laham, M. A.; Peng, C. Y.; Nanayakkara, A.; Gonzalez, C.; Challacombe, M.; Gill, P. M. W.; Johnson, B.; Chen, W.; Wong, M. W.; Andres, J. L.; Gonzalez, C.; Head-Gordon, M.; Replogle, E. S.; Pople, J. A. *Gaussian 98*, revision A.5; Gaussian, Inc.: Pittsburgh, PA, 1998.
- (56) (a) Gonzalez, C.; Schlegel, H. B. *J. Phys. Chem.* **1990**, *94*, 5523. (b) Bearpark, M. J.; Robb, M. A.; Schlegel, H. B. *Chem. Phys. Lett.* **1994**, *223*, 269.

The barrier to Berry pseudorotation (also see eq 3, Figure 3) is 8.1 kcal mol⁻¹, which confirms the CCSD(T)/6-31G**/B3LYP/6-31+G* result, 7.9 kcal mol⁻¹, via the C_{4v} transition state **2** (Table 1). An alternative transition state **3**, with C_s symmetry, has a 18.8 kcal mol⁻¹ relative energy with respect to **2** (Table 1).

In contrast to earlier RHF calculations on SF₄,¹⁹ the planar D_{4h} form **4** (Figure 1) has two imaginary frequencies (Table 1). The RHF solution for **4** is triplet unstable (see, e.g., ref 59), and the D_{4h} triplet ³A_{2u} state, **5**, at UB3LYP/6-31+G* is a minimum, 9.2 kcal mol⁻¹ lower in energy than the ¹A_{1g} singlet **4**. However, the geometry and energy of C_{3v} **6** (NIMAG = 2) is very close to that of **3** (Table 1). Density functional theory computations gave the ³A₁ C_{4v} structure at E_{rel} = 63.1 kcal

(57) Tolles, W. M.; Gwinn, W. D. *J. Chem. Phys.* **1962**, *36*, 1119.

(58) Kimura, K.; Bauer, S. H. *J. Chem. Phys.* **1963**, *39*, 3172.

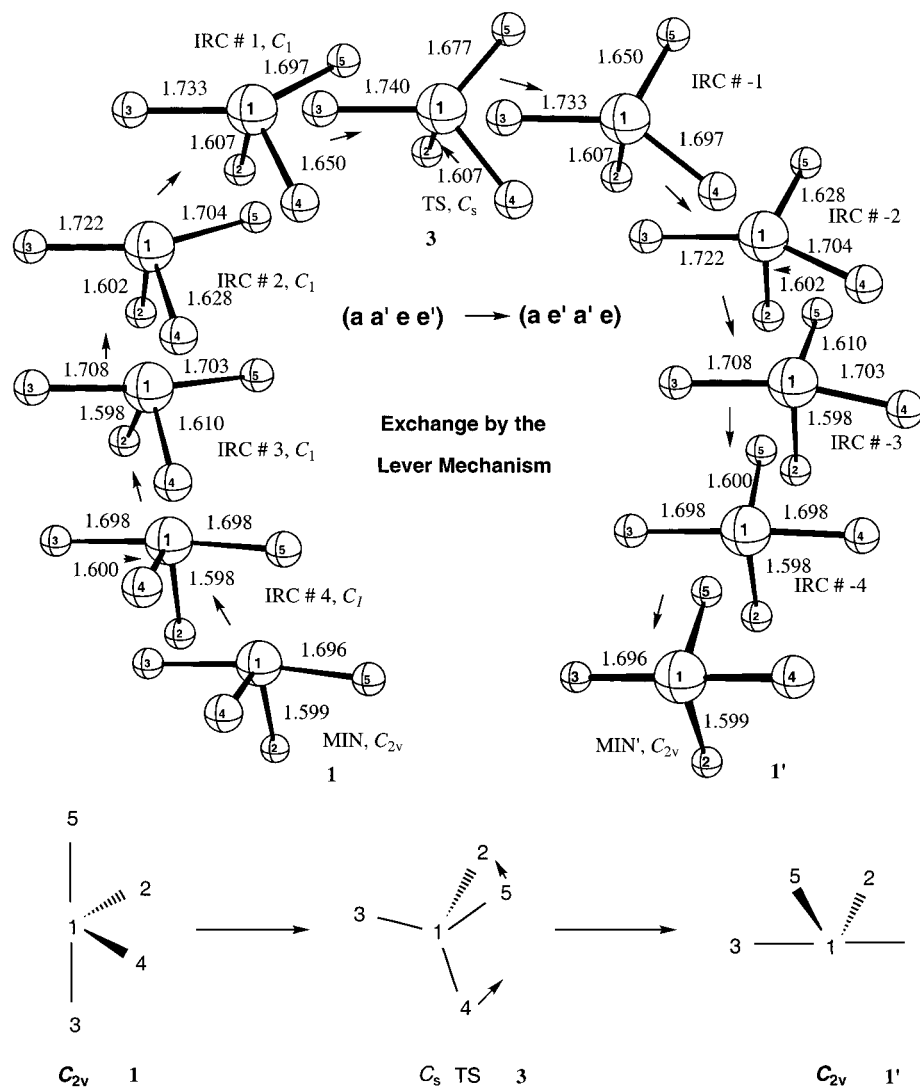


Figure 2. Illustration of the ligand permutation in SF₄ by the lever mechanism, as obtained from the IRC path. Several intermediate structures are shown together with their point group symmetries.

mol⁻¹ with respect to **1**.^{19b} Other stationary points on the singlet potential surface have more than one imaginary frequency and are all less stable than **3** (Table 1).⁶⁰ The geometry of the C_{3v} form, **7**, is close to tetrahedral (with one S–F bond extended), but T_d **8** is a third-order saddle point. Both **7** and **8** are lower in energy than **4** (Table 1).

Other stationary points reported earlier for the SF₄ and ClF₄⁺ potential energy surfaces include the D_{4h} form for SF₄ and the D_{4h} and T_d forms for ClF₄⁺, which were found to be much higher in energy (SF₄ D_{4h}, relative energy 108.8 kcal mol⁻¹ and NIMAG = 1 at HF/6-31G;⁶¹ ClF₄⁺ D_{4h}, NIMAG = 1, 59.5, T_d, NIMAG = 3, 138.0 kcal mol⁻¹,²⁷ both at the SCF/DZP level). Inversion in SF₄^{19a,25,26,61} and ClF₄⁺,²⁷ involving the (high-energy) D_{4h} structure, has been discussed.

Figure 2 shows some of the structures along the TS **3** IRC path. A wagging motion of the F₄–S₁–F₅ moiety with respect to the F₃–S₁–F₂ reference frame occurs, resulting in the shift of F₅ from an axial into an equatorial position (as the F₃–S₁–F₅ angle decreases). The F₃–S₁–F₂ angle remains virtually

unchanged. The same motion brings the originally equatorial ligand F₄ into an axial position, increasing the F₃–S₁–F₄ angle. All other bond angles and bond lengths adjust to these changes. Note that the originally equatorial ligand F₂ temporarily becomes apical in the transition state before it returns to an equatorial position, but one which is spatially inverted with respect to the initial position.

Figure 3 gives a schematic overview over the ligand permutational isomerism in penta- and tetracoordinated TBP or ψ -TBP compounds. The TR process, like BPR, results in a simultaneous exchange of two equatorial ligands with two axial ligands. The outcome of BPR and TR are different in asymmetrically substituted phosphoranes or related five-coordinated compounds, but simultaneous exchange of two axial–equatorial ligand pairs occurs in both mechanisms.²² In such pentacoordinated TBP molecules with five different ligands, an inversion of configuration is possible by a unique sequence of five BPR steps (with five different fixed points).²² Similar to BPR, TR results in five-step enantiomerization.²²

The initially equatorial vacant sites in a tetracoordinated TBP species always are the “fixed points” for Berry rotation, because structures with axial vacant sites are expected to be less stable.^{30,34} The fact that this does not result in complete

(59) Chambaud, G.; Levy, B.; Millie, P. *Theor. Chim. Acta* **1978**, *48*, 103.

(60) That C_{3v}, D_{2d}, and T_d symmetry structures are much higher in energy than the C_{4v} form also has been found for SH₄.^{3,15}

(61) Minyaev, R. M. *Russ. J. Inorg. Chem.* **1993**, *38*, 1300.

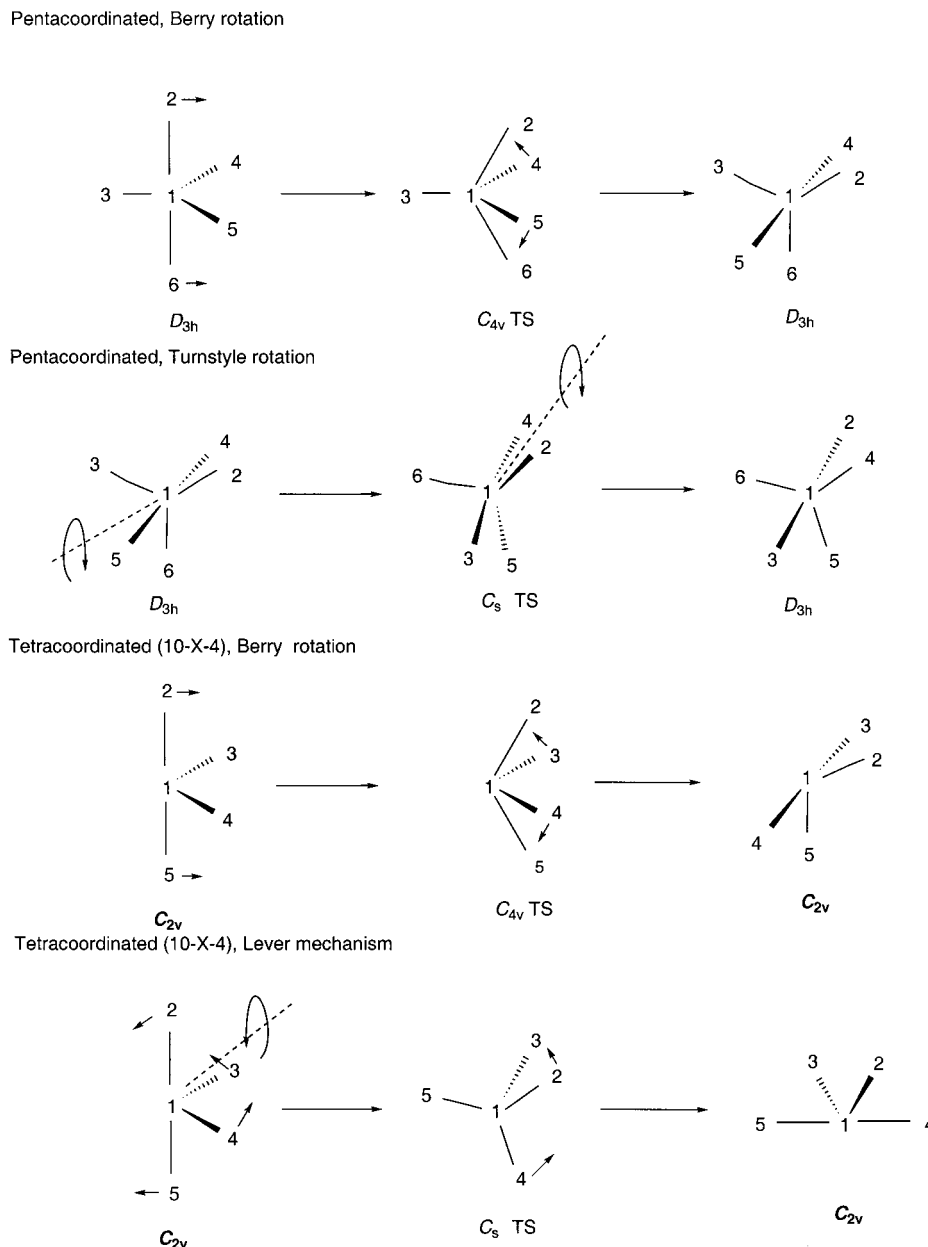


Figure 3. Schematic overview of BPR and lever processes in AX_4 compounds, as well as the BPR and TR processes in AX_5 molecules. BPR and TR in AX_5 molecules both result in double axial–equatorial exchange.

scrambling explains the lack of signal coalescence to a single F peak in the NMR spectrum of compound **d** (Scheme 1) and the absence of rapid racemization of compounds **a** and **b**.^{29,30,34}

The “lever” process (Figure 3), unlike the TR in pentacoordinated molecules, involves only a single exchange of one axial with one equatorial ligand, accompanied by an additional exchange of the resulting two equatorial positions. The lever process may bear some resemblance to the turnstyle rotation, because the topomerization might be described as a rotation of the ligand triple 2–3–4 (Figure 3, below) around a ψ -axis through the central atom, exchanging $2_{ax} \leftrightarrow 2_{eq}$, $4_{eq} \leftrightarrow 4_{ax}$ and $3_{eq} \leftrightarrow 3'_{eq}$, while keeping the 1–5 axis in a fixed frame. However, the actual IRC path (Figure 2) reveals that the lever mechanism is not similar to the turnstyle rotation in pentacoordinated systems.

Ugi et al.²² called such a hypothetical single-exchange process in pentacoordinated systems “M3” (named after Muetterties, who first conceived such a possibility⁶²). In five-coordinated species, M3 is tantamount to a sequence of two consecutive

TR steps, abbreviated as (TR)². However, M3 was ruled out by the Whitesides–Mitchell experiment, which precluded single axial–equatorial exchanges for five-coordinated phosphoranes.^{22a,63} Indeed, two consecutive TR rotations (with the vacant site as part of a ligand “pair”, rotating with regard to the rest of the molecule) would achieve the same ligand permutation as the lever mechanism in a single step. As a consequence, the lever mechanism in four-coordinated molecules involves only two possible reaction paths for every BPR process (with either one of the equatorial ligands becoming apical in the transition state); in contrast there are four equivalent TR processes in five-coordinated molecules.²²

The IRC (minimum energy) path for the lever process (Figure 4, Table A in the Supporting Information) is symmetric around the transition structure. E.g., angle F3–S1–F5 ($F3_{ax}$, $F5_{ax} \leftrightarrow$

(62) (a) Muetterties, E. L. *J. Am. Chem. Soc.* **1969**, *91*, 1636. (b) Also see a group theoretical treatment of this problem: Nourse, J. G. *J. Am. Chem. Soc.* **1977**, *99*, 2063.

(63) Whitesides, G. M.; Mitchell, H. L. *J. Am. Chem. Soc.* **1969**, *91*, 5384.

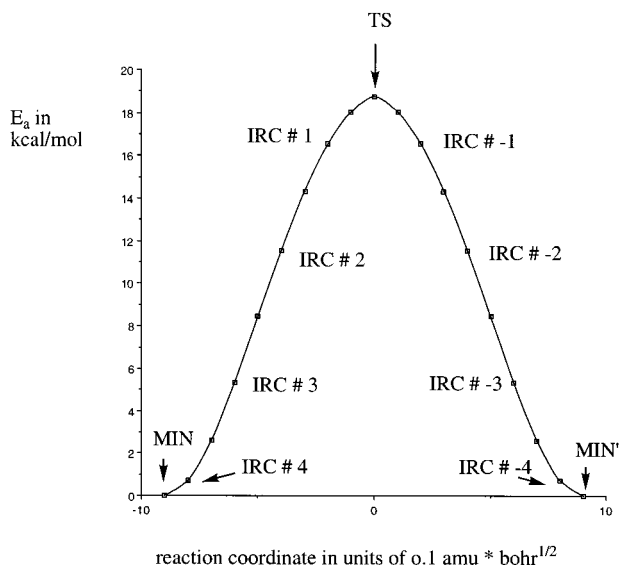


Figure 4. IRC path energy profile, symmetric around the transition state (vertical axis, energy of activation in kcal/mol; horizontal axis, reaction coordinate in $0.1 m_p^{1/2} a_0$).

$F3_{eq}$, $F5_{ax}$) exchanges its role with $F3-S1-F4$ ($F3_{ax}$, $F4_{eq} \leftrightarrow F3_{ax}$, $F4_{ax}$), and $F2-S1-F4$ exchanges its role with $F2-S1-F5$, both with one equatorial fluorine ($F2_{eq}$) and one axial fluorine ($F4_{ax}$, $F5_{ax}$).

Even an arbitrary sequence of the lever process does not lead to inversion of an AX_4 structure, as illustrated in Figure 5: an arbitrary sequence of three lever steps only generates the identity operation on the reactant structure. Intuitively, a sequence of single axial–equatorial exchanges acting first on one and then on the other axial ligand is anticipated to give the enantiomer of a chiral $SABCD$ or SA_2BC SF₄-like sulfurane or a related system. But as Figure 5 shows, any sequence of lever steps only leads back to the initial configuration, rather than to the enantiomer. To achieve not only full ligand scrambling but also inversion, a combination of one BPR with two lever steps is required. The two other possible combinations Berry–lever–lever and lever–Berry–lever lead to identical results.

SCl₂F₂. To elucidate the enantiomerization mechanisms in chiral sulfuranes, we have chosen a simple model, SCl₂F₂ (although experimentally unknown), for a PES search. Figure

6 shows 12 stationary points on the B3LYP/6-31+G* potential surface (see Table 2 for energies).

The $F_{ax}F_{ax}C_{2v}$ minimum **9** (Figure 6) is the most stable, in accord with the higher apicophilicity of fluorine with respect to chlorine.³⁴ But despite the apicophilicity rule, the energies of $F_{eq}F_{eq}$ **10** and the enantiomeric pair $F_{ax}F_{eq}$ **11** (2.2 and 2.4 kcal mol⁻¹ relative to **9**) are nearly the same.

Because of the inherently lower symmetry of SCl₂F₂ (than SF₄), there are in principle four different transition states for the lever process and two Berry rotation transition states (Figure 6). Two C_s TS's, **12** (with apical F, for $Cl_{ax} \leftrightarrow Cl_{eq}$ exchange) and **13** (with apical Cl, for $F_{ax} \leftrightarrow F_{eq}$ exchange) (Figure 6), are involved in the enantiomerization of **11** (verified by IRC calculations) by the lever process with 6.3 and 15.7 kcal mol⁻¹ barriers, respectively. The alternative interconversion of **11** and its enantiomer **11'** (with exchanges $F_{ax} \leftrightarrow F_{eq}$ and $Cl_{ax} \leftrightarrow Cl_{eq}$ occurring at the same time) by the BPR proceeds via the nonplanar C_s TS **14** with a barrier of 8.3 kcal mol⁻¹, close to that for the favored lever process. While direct inversion of **11** might proceed via planar C_{2v} **15**, this is 61.4 kcal mol⁻¹ higher in energy than **11** (Figure 6).

Achiral **9** and **10** are interconverted by the BPR process (by simultaneous $F_{ax} \leftrightarrow F_{eq}$ and $Cl_{ax} \leftrightarrow Cl_{eq}$ exchange), proceeding via a C_{2v} transition state **16** with $E_{rel} = 9.2$ kcal mol⁻¹ with respect to **9**. Only the lever mechanism interconverts the chiral $F_{ax}F_{eq}$ and the achiral $F_{ax}F_{ax}$ isomers via the C_1 TS **17** (with apical chlorine and $Cl_{eq} \leftrightarrow F_{ax}$ exchange) with a 17.8 kcal mol⁻¹ barrier with respect to **9**. An IRC calculation established the **9** \leftrightarrow **17** \leftrightarrow **11** pathway and ruled out the alternative **10** \leftrightarrow **17** \leftrightarrow **11** process.

We have been unable to locate the other conceivable C_1 transition structure for the $Cl_{ax} \leftrightarrow F_{eq}$ exchange and with apical F. On the basis of comparisons with the energies of C_s species **12** (F apical) and **13** (Cl apical, Table 2), this hypothetical C_1 TS should be lower in energy than **17**. The IRC calculations also confirmed that all three TBP C_s TS's **12**, **13**, and **17** correspond to the same type of lever permutation process, exemplified by TS **3** for SF₄.

There are two planar C_{2v} forms: **18** has two imaginary frequencies (Table 2) and is 11.6 kcal mol⁻¹ lower in energy than **15**. Species **19**, a planar conformation with D_{2h} symmetry (Figure 6), is even lower in energy and also has two imaginary

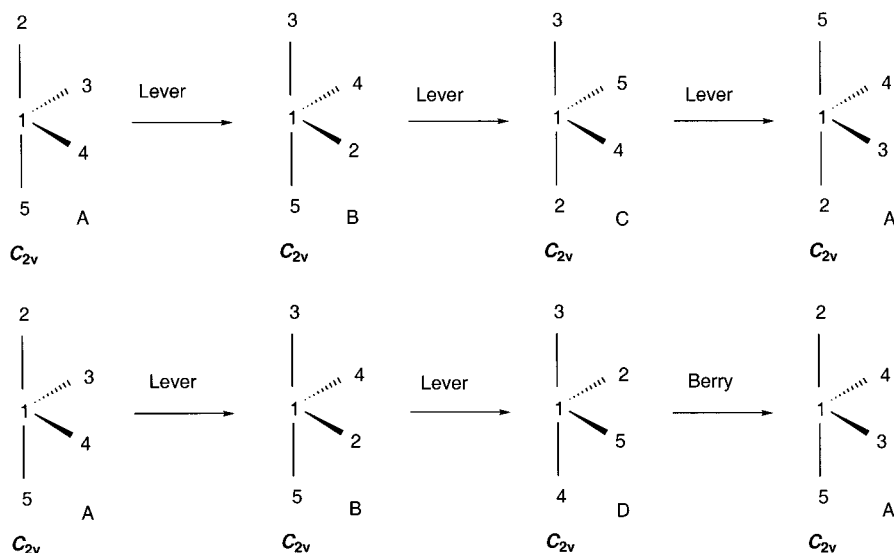


Figure 5. Three consecutive lever steps give the identity operation. Only a combination of one Berry with two lever steps permits enantiomerization of a chiral AX_4 TBP system.

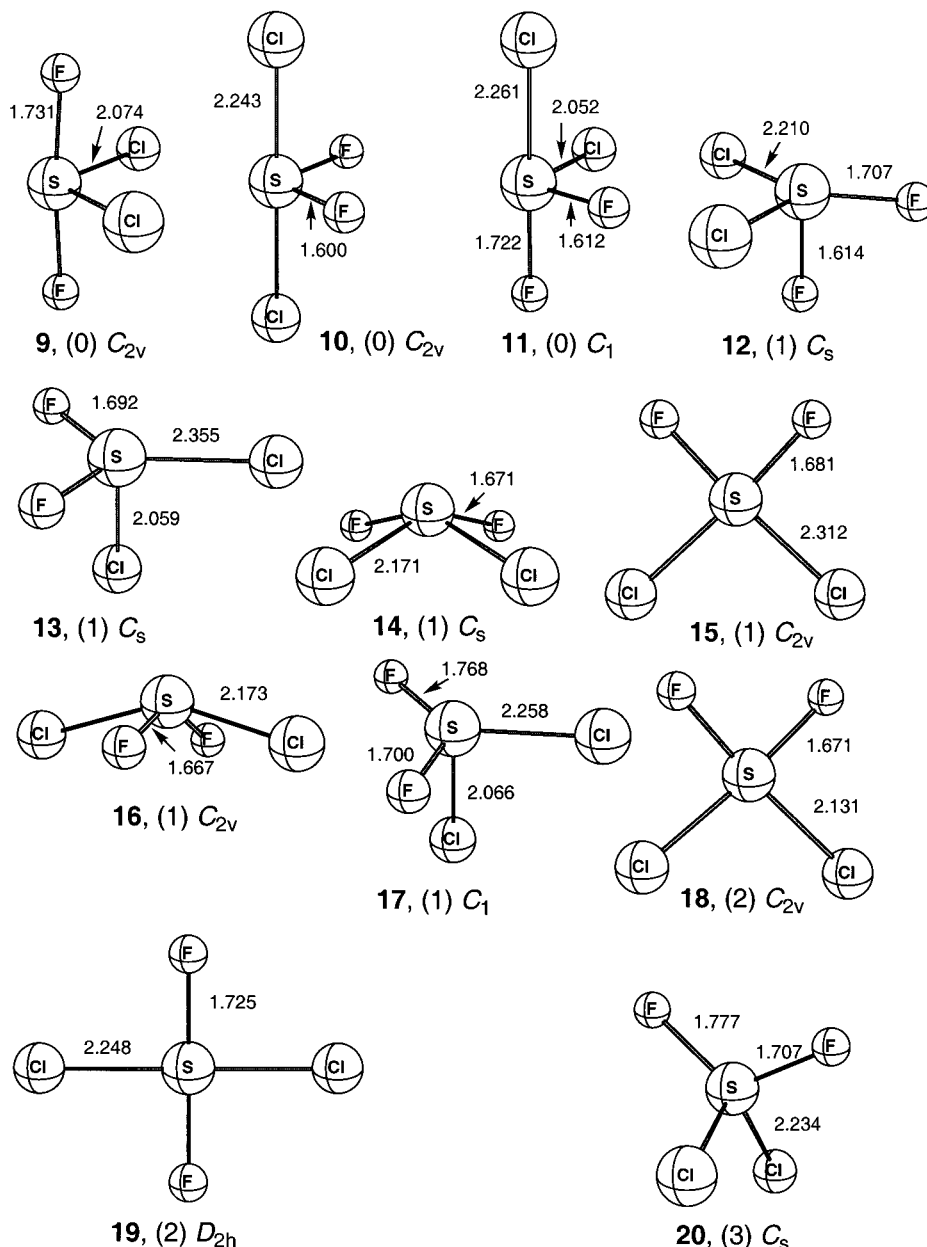


Figure 6. B3LYP/6-31+G* optimized structures of 12 stationary points on the SCl_2F_2 PES.

frequencies (Table 2). The nonplanar C_s form **20** (which resembles the T_d conformation **8** of SF_4) has three imaginary modes but is only $28.0 \text{ kcal mol}^{-1}$ less stable than **9**! Figure 7 displays all the reaction network possibilities corresponding to the transition structures we have located for topomerization in SCl_2F_2 schematically. Enantiomerization $\mathbf{11} \leftrightarrow \mathbf{11}'$ might occur in four different ways, among which, however, only the single Berry and one of the lever processes are competitive. In contrast to SF_4 , the barriers for Berry and for both lever mechanisms are low. Hence, SCl_2F_2 should racemize rapidly. This contrasts with the findings^{29,30} for dichloro-substituted **a** and **b** (Scheme 1), which are optically stable. This is only understandable if the replacement of the two fluorines in SCl_2F_2 by more electropositive ligands to give $\text{SCl}_2\text{RR}'$ results in a larger increase in the barrier of the lever process than in that for the Berry process.

The much higher activation barriers for the lever mechanism in sulfuranes than those for the Berry rotation (as in SF_4) explain the resistance of the known optically active sulfuranes, like **a** and **b**, to racemize, and of **f** to isomerize (Scheme 1).

Interhalogens. The C_{2v} global minimum of ClF_4^+ , **21** (Figure 8), first mentioned in 1968 on the basis of indirect evidence^{64a} and NMR spectroscopically characterized in 1973,^{64,65b} is iso-electronic and isostructural with SF_4 .^{64,65} We have found a TS **22** with C_s symmetry, with a geometry similar to the C_s TS in SF_4 and with a relative energy to the global minimum of $14.8 \text{ kcal mol}^{-1}$. An IRC calculation, starting from **22**, established the “lever mechanism” as being the process involved. However, the C_{4v} TS for Berry rotation, **23**, is much lower in energy ($2.5 \text{ kcal mol}^{-1}$, Table 3). The C_{3v} NIMAG = 2 species **24** is almost isoenergetic with the C_s TS ($\Delta E = 0.04 \text{ kcal mol}^{-1}$). The D_{4h} species **25** has two imaginary frequencies. One imaginary mode

(64) (a) Roberto, F. Q.; Mamantov, G. *Inorg. Chim. Acta* **1968**, 2, 317. (b) Christe, K. O.; Pilipovich, D. *Inorg. Chem.* **1969**, 8, 391 (c) Shamir, J. *Struct. Bonding* **1979**, 37, 141.

(65) (a) Christe, K. O.; Hon, J. F.; Pilipovich, D. *Inorg. Chem.* **1973**, 12, 84. (b) Christe, K. O.; Sawodny, W. *Inorg. Chem.* **1973**, 12, 2879. (c) Christe, K. O.; Sawodny, W. 6th International Symposium on Fluorine Chemistry, Durham, England, July 1971. (d) Stein, L. In *Halogen chemistry* Gutmann, V., Ed.; Academic Press: London, 1967; Vol. 1, pp 133–224.

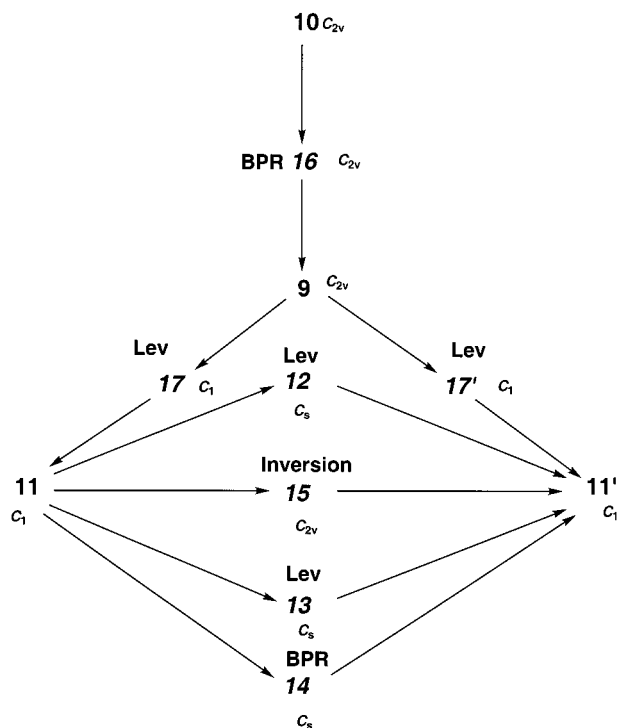


Figure 7. Schematic representation of the reaction path network in the SCl₂F₂ system.

(−992.5 cm^{−1}) connects two enantiomeric (inverted) BPR TS's (Figure 9). The other (−90.9 cm^{−1}) leads to a *D*_{2d} structure **26** (Figure 8), 7.4 kcal mol^{−1} lower in energy than **25**.⁶⁶

The results for BrF₄⁺,⁶⁵ first mentioned speculatively in 1967^{65d} and tentatively characterized in 1971,^{65c} are similar to those for ClF₄⁺ (Figure 8 and Table 3) and include a *C*_{2v} minimum **27**, a *C*_s “lever” TS **28**, a BPR *C*_{4v} TS **29**, and a *D*_{4h} second-order saddle point **30**. The barriers are 11.3 kcal mol^{−1} for the lever process and 4.7 kcal mol^{−1} for the Berry rotation, while the *D*_{4h} form relative energy is quite high, 76.3 kcal mol^{−1}.

In contrast to the SCl₂F₂ system, no bound BrF₂Cl₂⁺ stationary points (Table 3) with two anti or two apical chlorine atoms could be located; this drastically reduces the number of species (and possible topomerization routes). There are only three minima, *C*_{2v} **31** (F_{ax}F_{ax}) and a *C*₁ enantiomeric pair **32** (F_{ax}F_{eq}). Two lever mechanism transition states exist, one *C*_s form **33** for F_{ax} ↔ F_{eq} exchange (for the **32** ↔ **32'** enantiomerization) and one *C*₁ transition state **34** for the **31** ↔ **32** interconversion (F_{ax} ↔ Cl_{eq} exchange). With the heavier halogen ligands, the preference of the Berry over the lever mechanism diminishes; the Berry rotation TS (for enantiomerization of **32** by simultaneous F_{ax} ↔ F_{eq} and Cl_{ax} ↔ Cl_{eq} exchange) is found to be only 2.8 kcal mol^{−1} lower in energy than the lever TS **33** (Table 3). Remarkably, the relative energy of the planar *D*_{4h} form **36** with NIMAG = 2 is only 36.0 kcal mol^{−1} with respect to **31**.

PF₄[−]. The tetrafluorophosphate anion, prepared by the reaction of [N(CH₃)₄]⁺F[−] and PF₃ in excess PF₃ as the solvent,

also was studied computationally by the same authors.²¹ The potential energy surface of PF₄[−] (Table 4, Figure 9) is similar to that of the isoelectronic SF₄ (Figure 1, Table 1) and ClF₄⁺ and BrF₄⁺ (Figure 8, Table 3). The global minimum is again a *C*_{2v} structure (**37**, Figure 10). The difference in the activation barriers for the lever process in PF₄[−] (*C*_s TS **38**, 16.1 kcal mol^{−1}) and the Berry process (*C*_{4v} TS **39**, 9.3 kcal mol^{−1}) is much smaller, if compared to the situation in SF₄ and in the AF₄⁺ interhalogen cation examples (Tables 1, 3, and 4). Species **40** is a TBP *C*_{3v} form with two imaginary frequencies, only 1.1 kcal mol^{−1} higher in energy than TS **38**, while *D*_{4h} **41** is much higher in energy (Table 4) and also has two imaginary frequencies. But instead of the *D*_{2d} form **26** in ClF₄⁺, there is a *T*_d form **42**, similar to that in SF₄ and lower in energy than **41**.

Christe et al.²¹ found a barrier to the BPR process in PF₄[−] of 10.2 kcal mol^{−1} at the MP2/DZP level, somewhat higher than our value and in better agreement with experiment (10.3 kcal mol^{−1} ⁴²).

Trends in Lever and Berry Activation Barriers. In order to reveal possible trends in the activation energies for the alternative lever and Berry processes, we have compared the relative energies of the *C*_{2v}, *C*_{4v} (Berry TS), *C*_{3v}, and *C*_s (lever TS) stationary points for the series PF₄[−], AsF₄[−], SbF₄[−], SbCl₄[−], SF₄, SeF₄, TeF₄, ClF₄⁺, BrF₄⁺, IF₄⁺ (Table 5 and Figure 11). The activation barriers for both Berry and lever mechanisms decrease down the group, with the exception of the interhalogens. Going from the left to the right in the periodic table, the preference of the Berry mechanism increases.

Increasing the number of chlorine ligands disfavors the Berry process (Tables 2, 3 and 5), depending on the central atom. While in BrF₂Cl₂⁺, the Berry mechanism is still preferred, the barriers for the lever and the Berry process become nearly equal for SCl₂F₂, whereas for SbCl₄[−] the lever mechanism is favored.

While the energy difference between the *C*_s lever TS's and the *C*_{3v} structures also diminishes with the heavier elements (Table 5), the nature of the *C*_{3v} form changes from a second-order saddle point for the lighter elements to a minimum for the heaviest systems. In IF₄⁺, the energies of the *C*_{2v} (minimum) and *C*_{4v} (transition state) become virtually identical. However, at a different level of theory^{52,53} we have found IF₄⁺ in *C*_{4v} to be 1.4 kcal mol^{−1} higher in energy than in *C*_{2v} (Table 5).

Effective Monkey Saddle Points in AX₄ Species. Gradient lines connect the *C*_{3v} structures with three lever (*C*_s) transition states (which are either second-order saddle points, Figure 12, or minima, Figure 13), reached by only small distortions (like the letter Y) of the equatorial bonds. This situation has been described earlier for ClF₄⁺²⁷ and for ClF₃.⁶⁷ According to our computations (Table 5), the energy difference between the *C*_s and the *C*_{3v} structures becomes as small as 0.04 kcal mol^{−1}, even without ZPE correction (IF₄⁺, where the *C*_{3v} minimum lies in a deeper trough, is an exception). An idealization of the PES around the central *C*_{3v} form is illustrated in Figure 14, showing three valleys that meet on a hilltop. This is called a “monkey saddle”.⁶⁸ A monkey saddle point with three valleys is characterized by the absence of any negative curvature and a doubly degenerate zero eigenvalue of the Hessian (i.e., a degenerate zero frequency).⁶⁹ Indeed, we have found very small doubly degenerate real or imaginary frequencies (typically below 50 cm^{−1}) for the *C*_{3v} geometries of these AX₄ species. But as these stationary points fall just short of meeting the mathematical

(66) These findings do not agree with earlier work^{27,61} which appears to be an artifact probably arising from the instability of the wave function. The reported MP2/DZP data^{27,61} differs tremendously from our results, e.g., *D*_{4h} ClF₄⁺ was claimed to be the global minimum (!), 16.2 kcal mol^{−1} lower in energy than the *C*_{2v} form, and *C*_{3v} ClF₄⁺ was reported to be 65.3 kcal mol^{−1} higher in energy than the closely related *C*_s “lever” transition state! We found two apparent *D*_{4h} stationary points, one with a short and the other, low in energy, with a longer Cl–F distance at both MP2/6-311+G* and B3LYP/6-311+G*. Both *D*_{4h} forms were unstable at both levels, and the *C*_{3v} form is stable.

(67) Minyaev, R. M. *Chem. Phys. Lett.* **1992**, *196*, 203.

(68) Mezey, P. *Potential Energy Hypersurfaces*; Elsevier: New York, 1987.

(69) Valtazanos, P.; Ruedenberg, K. *Theor. Chim. Acta* **1986**, *69*, 281.

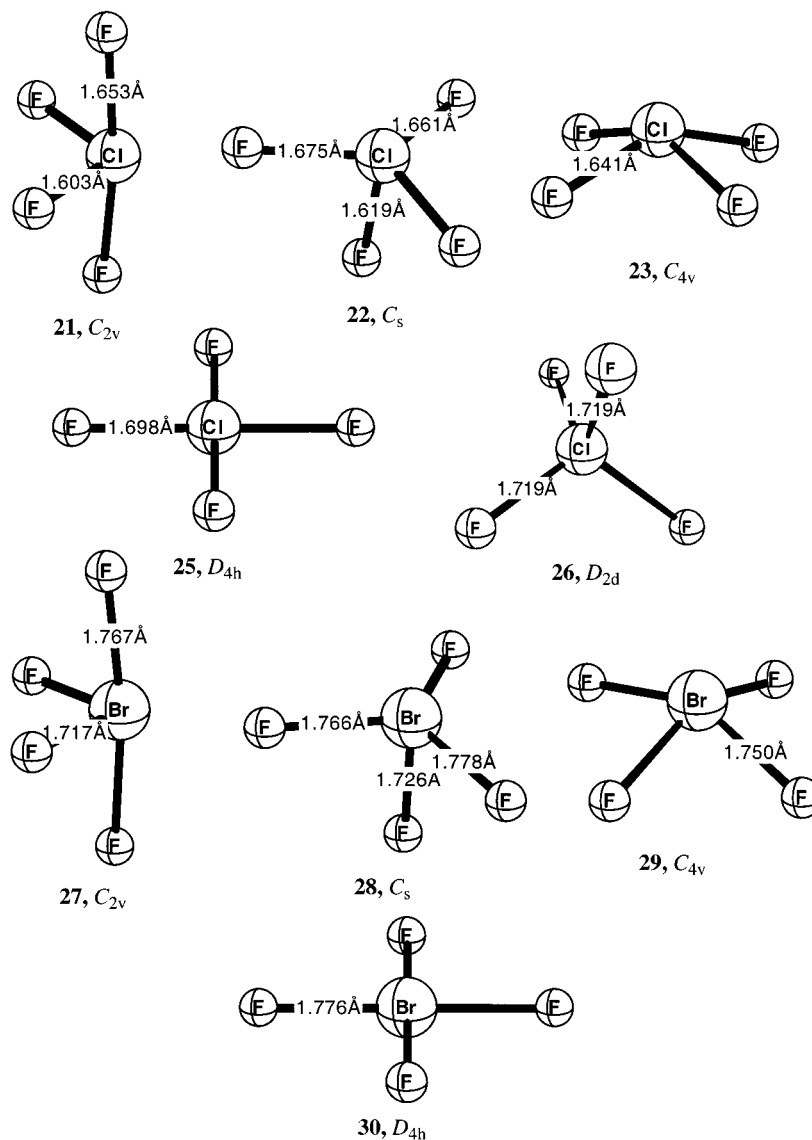


Figure 8. B3LYP/6-31+G* optimized structures of the stationary points on the ClF_4^+ and BrF_4^+ potential surfaces, related to the discussion of the lever process.

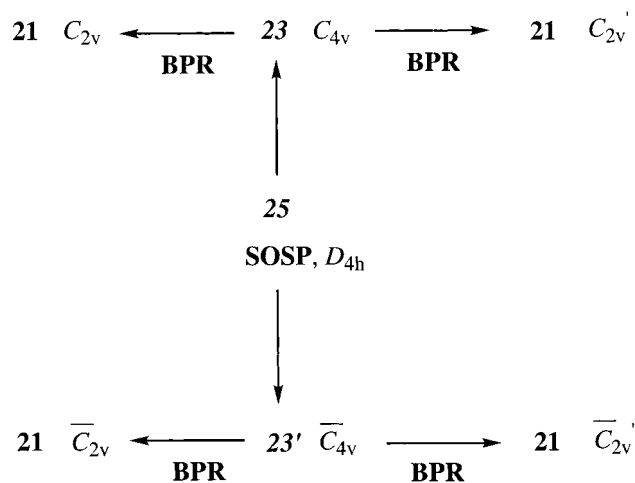


Figure 9. Gradient lines pertaining to the conical inversion of the C_{2v} minima in interhalogen cations (exemplified by ClF_4^+ and SF_4) via the D_{4h} structure. The second-order saddle point (SOSP) in the center connects to the two inverted forms of **23**, the Berry rotation TS's.

conditions for a “monkey saddle” (i.e., exactly zero frequencies), we prefer the term “effective monkey saddle point” to describe

them. The “minimum energy paths” either encircle the effective monkey saddle point (Figure 12) or pass right through it, since, at least approximately, the reaction path branches there (Figure 13). An IRC run on the ClF_4^+ MP2/6-31G PES (with a C_{3v} minimum) approached the extremely shallow central “minimum”, only 10^{-5} hartree lower in energy than the C_s “transition state”.

The minimum energy path originating from one C_{2v} minimum (Figure 13) will proceed without any significant barrier toward either of the two other C_{2v} minima, once the branching point at the C_{3v} hilltop is passed. Hence, the C_{3v} form can be regarded as the “transition state” for the reaction, coinciding with a bifurcation.⁶⁹ A monkey saddle point apparently would violate the Murrell–Laidler theorem⁷⁰ and the McIver–Stanton rules.⁷¹ The controversy about the existence of monkey saddle points in chemistry goes back to Murrell and Laidler’s work in 1967,⁷⁰ which ruled out the possibility of “three valleys meeting at a hilltop” on the basis of the harmonic approximation.⁷⁰ This viewpoint was challenged in 1974 by Stanton and McIver by

(70) Murrell, J. N.; Laidler, K. J. *Trans. Faraday Soc.* **1968**, *64*, 371.

(71) (a) Stanton, R. E.; McIver, J. W. *J. Am. Chem. Soc.* **1975**, *97*, 3632.

(b) McIver, J. W. *Acc. Chem. Res.* **1974**, *7*, 72.

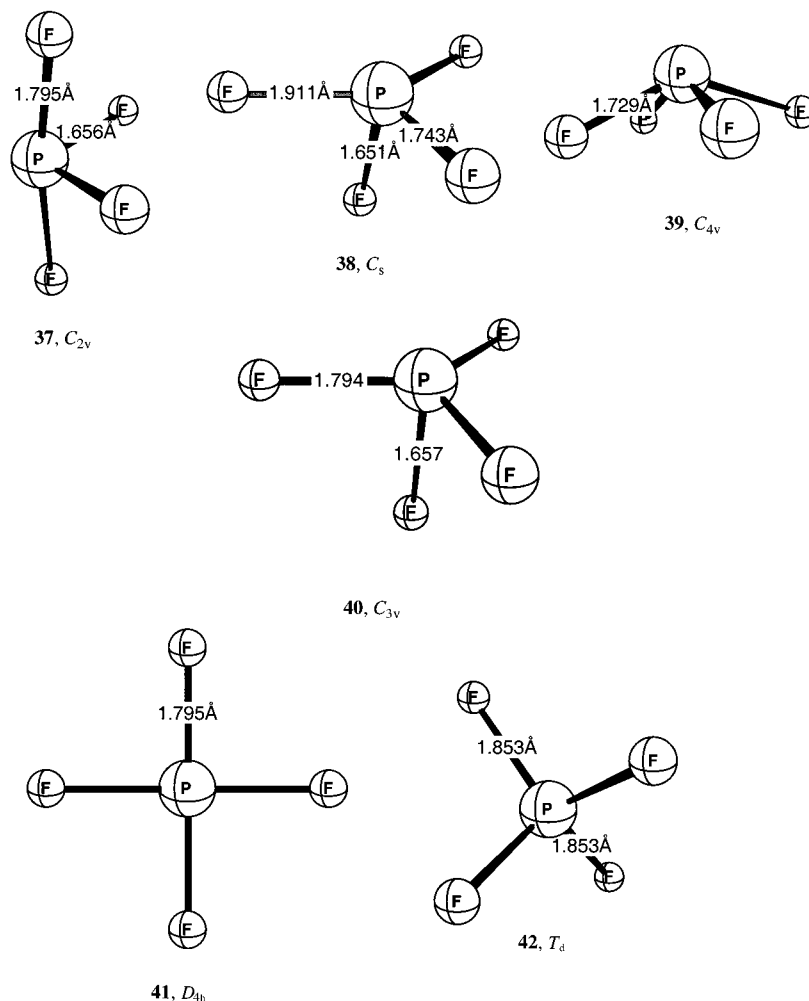


Figure 10. The B3LYP/6-31+G* optimized structures of the tetrafluorophosphate anion PF₄⁻. Note the similarity to the isoelectronic forms of SF₄ and ClF₄⁺.

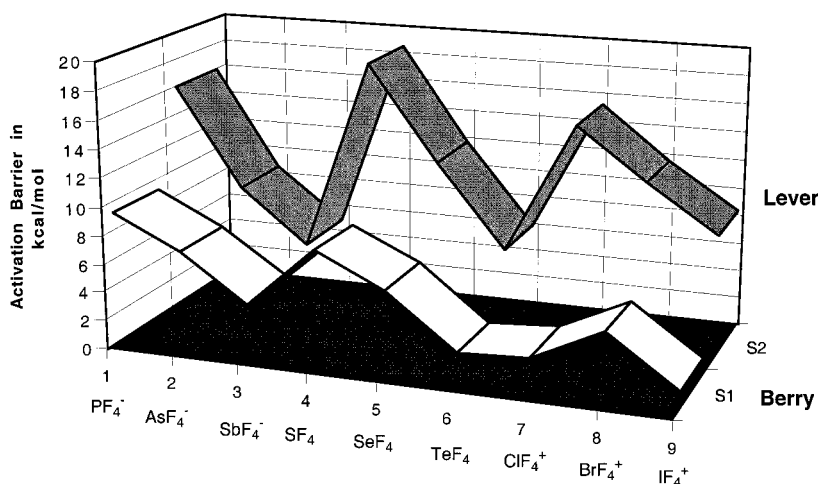


Figure 11. Trends in the activation energy barriers for the Berry (lighter ribbon) and lever (darker ribbon) mechanisms in AF₄ species.

taking cubic and higher order terms into account in describing the potential surface at a “monkey saddle”.⁷¹ They even considered “monkey saddles” with four valleys, in which case even the cubic, and not only the quadratic, terms vanish.⁷¹ Stanton and McIver maintained that “it would be an unlikely numerical accident if an eigenvalue (of the Hessian) should be exactly zero at such a (stationary) point”.⁷¹ We argue that small changes in cases where an effective monkey saddle point already is present, e.g., by changing the basis set in a quantum-chemical

computation, or by very small variations in the ligand groups, might allow such an “accident” to be approached very closely. The usual harmonic approximation for the calculation of vibrational frequencies is not appropriate for such systems, because quadratic terms are absent in the description of the potential surface at the central point. Hence, small variations in the level of theory might change the nature of the C_{3v} structure from a minimum into a second-order saddle point, or vice versa. More recently, Wales and Berry⁷² demonstrated that in high-

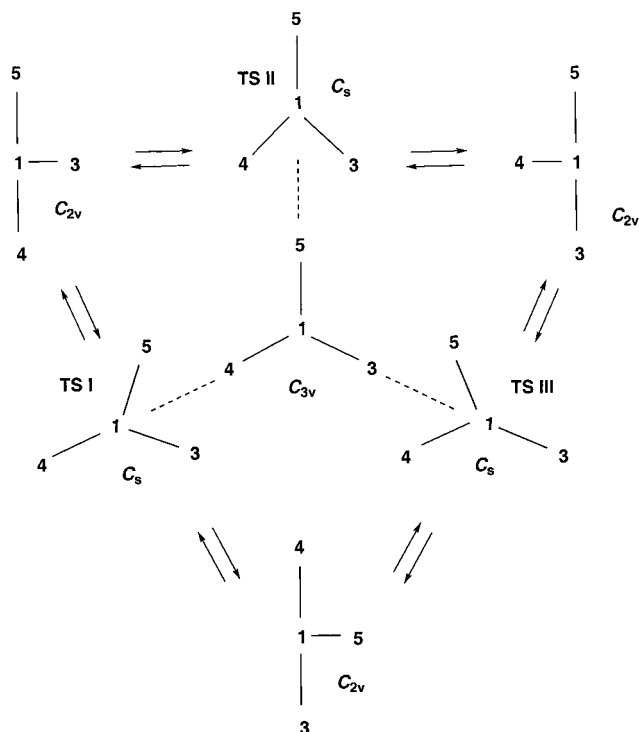


Figure 12. Schematic illustration of the “effective monkey saddle points” when the central C_{3v} structure has two imaginary frequencies (the bond to the fourth ligand 2 is perpendicular to the projection plane).

symmetry cases, such “as second order Jahn-Teller points or transition states at points of three-fold or higher symmetry”, the “effective potential energy function fails to satisfy the conditions required for the Murrell-Laidler theorem to hold.”^{72,73} They concluded that it is possible to find potential surfaces with transition states connecting three or more potential minima.⁷²

Several examples of monkey saddle points have been proposed^{74–77} involving “forbidden”⁷¹ transition states that violate the Stanton–McIver symmetry rule; i.e., that “no structure can serve as a transition state for a given reaction if a C_3 rotation or other odd degree symmetry operation associated with the structure converts reactants into products”.⁷¹ In 1976, Pechukas deliberately ignored the “weird possibility” of a monkey saddle in extending Stanton and McIver’s work to derive more stringent rules governing the allowed symmetries for transition states.⁷⁸ The most recent example is the 4-fold monkey saddle point described by Li and Houk.⁷⁷ This is involved in the syn dimerization of two cyclobutadienes which gives four equivalent products. The D_{4h} saddle point has two imaginary vibrational modes corresponding to two degenerate asynchronous concerted [4 + 2] cycloadditions, but the steepest descent is along four equivalent paths on the PES in the directions of the dimer minima. Cremer discussed a monkey saddle in 1993 on the barbaralyl cation ($C_9H_9^+$) PES, where a D_{3h} structure is connected by six equivalent downhill paths to six equivalent C_s minima.⁷⁶

Because “effective monkey saddle points” are, for all practical purposes, the lowest maxima on the minimum energy paths

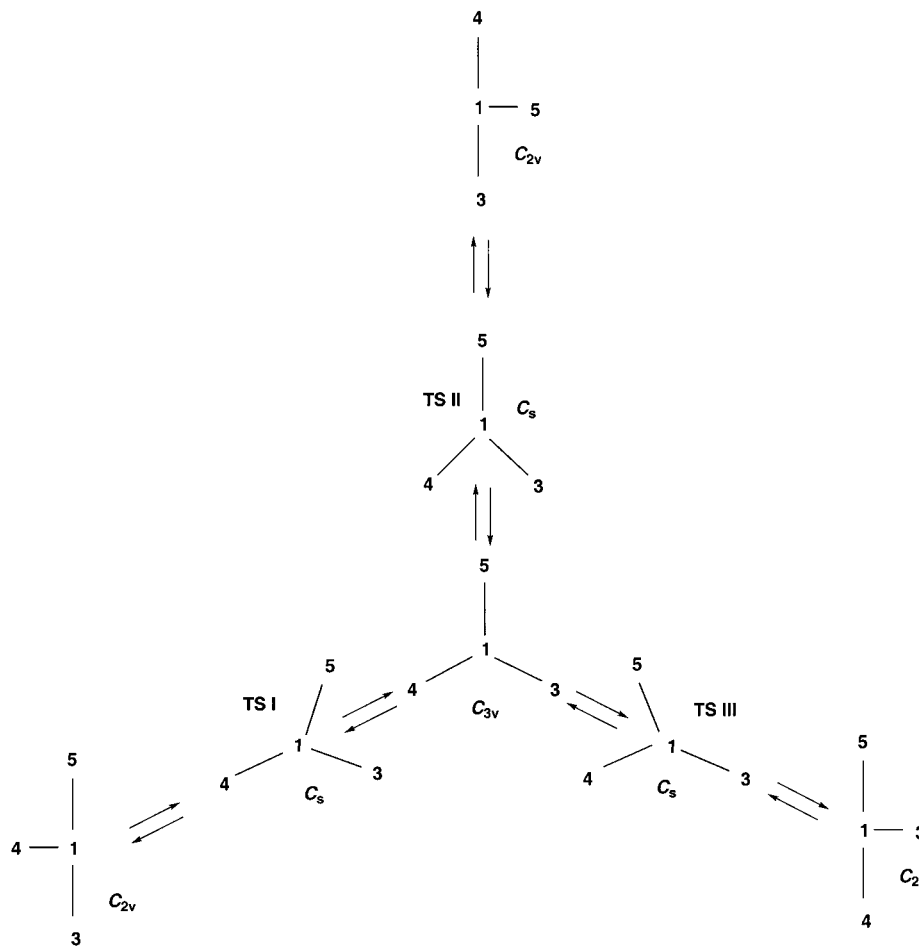


Figure 13. Schematic illustration of the minimum energy paths, connecting permutational isomers of AX_4 species, which pass through a central C_{3v} minimum, the “effective monkey saddle” branching point.

**PES in the neighborhood of a monkey saddle point
with three valleys, defined by $z(x,y) = x^3 - 3xy^2$**

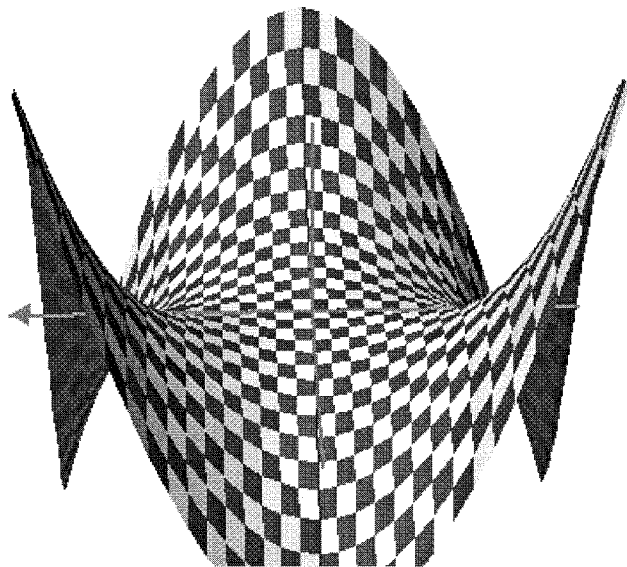


Figure 14. Perspective representation of the functional form of the ideal monkey saddle.

connecting reactants to products, we suggest a revision of the rules^{71,78} for the allowed point group symmetries of transition states.

4. Conclusions

While the Berry mechanism is preferred in SF₄ and all isoelectronic AF₄ systems, the lever process is required for the enantiomerization of chiral isomers of SCl₂F₂. The lever mechanism provides the only means to exchange achiral F_{ax}F_{ax} or F_{eq}F_{eq} isomers with the chiral F_{ax}F_{eq} forms. Interhalogen cations (Table 3, Figure 8) and the PF₄⁻ anion (Table 4, Figure 10) behave like SF₄ and SCl₂F₂ and have similar potential energy surface topographies.

Both Berry and lever activation barriers in AF₄ species (Figure 11) decrease down the group. The only AX₄ system which

showed a strong preference for the lever mechanism is SbCl₄⁻. Other ACl₄ systems also might favor the lever mechanism.

Chiral halosulfuranes such as **a**, **b**, and **c** in Scheme 1 or related systems, like chiral periodonium ions,⁷⁹ or chiral four-coordinated transition metal complexes with a “saw horse” structure, like RuHClL₂ (L = PⁱPr₃),⁸⁰ are in principle capable of enantiomerization via a combination of a single Berry pseudorotation and two lever steps (Figure 5). The necessity of including lever steps in the enantiomerization mechanism explains the optical stability of chiral halosulfuranes where higher activation barriers are involved.

Remarkably, the C_{3v} and the C_s (lever transition state) structures are almost isoenergetic for all AX₄ systems studied (Table 5). The C_{3v} forms have either (1) two very small degenerate imaginary or (2) real frequencies, the two lowest of which are very small. In the former case, the minimum energy lever path encircles a second-order saddle point in triangular fashion (Figure 12), while in the second case the C_{3v} structure lies in an extremely shallow potential well on the minimum energy path, connecting two equivalent global minima (Figure 13).

The corresponding potential surface topography, the “effective monkey saddle point”, can be described as three valleys on a corrugated surface that meet at a hilltop. Both these cases approximate the topological monkey saddle, which is characterized by the absence of any negative curvature, but with two degenerate (exactly) zero eigenvalues of the Hessian (i.e., zero frequencies).⁶⁹

According to the Stanton–McIver theorems,⁷¹ monkey saddles such as those described in this work are precluded as transition states. Our findings suggest that an ideal monkey saddle can be approached to a high degree of approximation by an effective monkey saddle point adjusted by small variations in the chemistry, e.g., alterations in a ligand chain, that only will result in negligible deviations from the local symmetries at the central atom. As a consequence, the effective monkey saddle point becomes for all practical purposes the transition state of a chemical reaction. Hence, we suggest an amendment in the accepted rules extending the allowed symmetries of transition states.

Acknowledgment. We thank the Deutsche Forschungsgemeinschaft (DFG) for financial support, Prof. Oleg Charkin (Moscow) for his interest, and Prof. Wesley Allen (Athens, GA) for a suggestion.

Supporting Information Available: Table A containing bond angle data of intermediate structures along the IRC path. This material is available free of charge via the Internet at <http://pubs.acs.org>.

IC990500X

(72) Wales, D. J.; Berry, R. S. *J. Chem. Soc., Faraday Trans.* **1992**, *88*, 543.

(73) One of the referees remarked that we might have overlooked “Jahn–Teller effects as the possible driving force behind the frequent occurrence of C_{3v} stationary points with degenerate imaginary frequencies”. The referee suggested that the C_{3v} HOMOs might be half-filled degenerate molecular orbitals. This is not the case. Moreover, our wave function stability calculations on the C_{3v} forms of ClF₄⁺ and SF₄ showed the absence of singlet or triplet instabilities for both closed-shell species. We cannot preclude that the structures discussed in our work as effective monkey saddles are second-order Jahn–Teller points involving closely lying MOs.⁸¹

(74) Stohrer, W. D.; Hoffmann, R. *J. Am. Chem. Soc.* **1972**, *94*, 1661.

(75) Hay, P. J.; Goddard, W. A. *Chem. Phys. Lett.* **1972**, *14*, 46.

(76) Cremer, D.; Svensson, P.; Kraka, E.; Ahlberg, P. *J. Am. Chem. Soc.* **1993**, *115*, 7445.

(77) Li, Y.; Houk, K. N. *J. Am. Chem. Soc.* **1996**, *118*, 880.

(78) Pechukas, P. *J. Chem. Phys.* **1976**, *64*, 1516.

(79) Dess, D. B.; Wilson, S. R.; Martin, J. C. *J. Am. Chem. Soc.* **1993**, *115*, 2488.

(80) Coalter, J. N., III; Spivak, G. J.; Gerard, H.; Clot, E.; Davidson, E. R.; Eisenstein, O.; Caulton, K. G. *J. Am. Chem. Soc.* **1998**, *120*, 9388.

(81) Burdett, J. K. *Molecular Shapes*; Wiley: New York, 1980; Chapter 5.